Non-equilibrium quench dynamics in quantum quasicrystals

2013 New J. Phys. 15 023036

(http://iopscience.iop.org/1367-2630/15/2/023036)

New Journal of Physics
The open access journal for physics

Non-equilibrium quench dynamics in quantum quasicrystals

Ferenc Iglói[1,2], Gergő Roósz[1,2] and Yu-Cheng Lin[3]

[1] Wigner Research Centre, Institute for Solid State Physics and Optics, PO Box 49, H-1525 Budapest, Hungary
[2] Institute of Theoretical Physics, Szeged University, H-6720 Szeged, Hungary
[3] Graduate Institute of Applied Physics, National Chengchi University, Taipei, Taiwan
E-mail: igloi.ferenc@wigner.mta.hu, gergo_roosz@titan.physx.u-szeged.hu and yc.lin@nccu.edu.tw

New Journal of Physics **15** (2013) 023036 (20pp)
Received 26 October 2012
Published 25 February 2013
Online at http://www.njp.org/
doi:10.1088/1367-2630/15/2/023036

Abstract. We study the non-equilibrium dynamics of a quasiperiodic quantum Ising chain after a sudden change in the strength of the transverse field at zero temperature. In particular, we consider the dynamics of the entanglement entropy and the relaxation of the magnetization. The entanglement entropy increases with time as a power law, and the magnetization is found to exhibit stretched-exponential relaxation. These behaviors are explained in terms of anomalously diffusing quasiparticles, which are studied in a wave packet approach. The non-equilibrium magnetization is shown to have a dynamical phase transition.

Contents

1. Introduction

The recent experimental progress in ultracold atomic gases in optical lattices [1–10] has opened up fascinating new perspectives on research in the field of isolated quantum systems, both in equilibrium and out of equilibrium. In experiments, the form of atomic interactions can be suddenly changed by tuning an applied magnetic field near a Feshbach resonance, which is known as a global quantum quench. On the theoretical side, one is interested in the time evolution of different observables, such as the order parameter or some correlation function, after a quench. The fundamental questions concerning quantum quenches include (i) the functional form of the relaxation process in early times and (ii) the properties of the stationary state of the system after a sufficiently long time.

Many results for quantum quenches have been obtained for *homogeneous* systems [11–32]; for example, the relaxation of correlation functions in space and time is generally in an exponential form, which defines a quench-dependent correlation length and a relaxation (or decoherence) time. Many basic features of the relaxation process can be successfully explained by a quasiparticle picture [14, 33, 34]: after a global quench quasiparticles are created homogeneously in the sample and move ballistically with momentum-dependent velocities. The behavior of observables in the stationary state is generally different in integrable and non-integrable systems. For non-integrable models, thermalization is expected [12–22] and the distribution of an observable is given by a thermal Gibbs ensemble; however, in some specific examples this issue has turned out to be more complex [23–25, 31]. By contrast, it was conjectured that stationary state averages for integrable models are described by a generalized Gibbs ensemble [12], in which each integral of motion is separately associated with an effective temperature.

Concerning quantum quenches in inhomogeneous systems, there have been only a few studies in specific cases; for example, entanglement entropy dynamics in random quantum chains [35–37] and in models of many-body localization [38, 39]. In some of these cases the eigenstates are localized, which prevents the system from reaching a thermal stationary state.

A special type of inhomogeneity, interpolating between homogeneous and disordered systems, is a quasicrystal [40, 41] or an aperiodic tiling [42]. Quasicrystals are known to have anomalous transport properties [43, 44], which is due to the fact that in these systems the long-time motion of electrons is not ballistic, but an anomalous diffusion described by a power law. One may expect that the quasiparticles created during the quench have a similar dynamical behavior, which in turn affects the relaxation properties of quasicrystals.

Quasicrystals of ultracold atomic gases have been experimentally realized in optical lattices by superimposing two periodic optical waves with different incommensurate wavelengths. An optical lattice produced in this way realizes a Harper's quasiperiodic potential [47, 48], for which the eigenstates are known to be either extended or localized depending on the strength of the potential. Different phases of the Bose–Hubbard model with such a potential have been experimentally investigated [45, 46]. There have also been theoretical studies concerning the relaxation process in the Harper potential [49, 50].

In this paper, we consider the non-equilibrium quench dynamics of the quantum Ising chain in one-dimensional quasicrystals. The quantum Ising chain in its homogeneous version is perhaps the most studied model for non-equilibrium relaxation [34, 51–66]. Our study extends previous investigations in several respects and seeks to obtain new insights into quench dynamics in inhomogeneous systems. We focus on the Fibonacci lattice, for which many equilibrium properties of the quantum Ising model are known [67–73]; to our knowledge, this is the first study of quantum quenches in such a lattice. Using free-fermionic techniques [75], we numerically calculate the time dependence of the entanglement entropy as well as the relaxation of the local magnetization for large lattices. The numerical results are interpreted by a modified quasiparticle picture, in which the quasiparticles are represented by wave packets; we also obtain diffusive properties of the wave packets.

The structure of this paper is as follows. The quasiperiodic quantum Ising model and its equilibrium properties are described in section 2. The global quench process and some known results for homogeneous and random chains are presented in section 3. Our numerical results for the quasiperiodic chain are presented and interpreted in section 4. This paper is concluded with a discussion; some details of the free-fermionic calculation of the local magnetization are presented in the appendix.

2. The model and its equilibrium properties

We consider the quantum (or transverse) Ising model defined by the Hamiltonian

$$\mathcal{H} = -\frac{1}{2}\left[\sum_i J_i \sigma_i^x \sigma_{i+1}^x + h \sum_i \sigma_i^z\right], \tag{1}$$

where σ_i^x and σ_i^z are Pauli matrices at site i. The interactions, J_i, are generally site dependent, which are parameterized as

$$J_i = J r^{f_i}, \tag{2}$$

where $r > 0$ is the amplitude of the inhomogeneity, and the integers f_i are taken from a quasiperiodic sequence.

Quasiperiodic lattices can be generated in different ways, such as by the cut-and-project method. Here, we use the following algebraic definition for a one-dimensional quasiperiodic sequence:

$$f_i = 1 + \left[\frac{\mathrm{i}}{\omega}\right] - \left[\frac{\mathrm{i}+1}{\omega}\right], \tag{3}$$

where $[x]$ denotes the integer part of x and $\omega > 1$ is an irrational number. The Fibonacci sequence generated by the substitution rule: $0 \to 01$ and $1 \to 0$ starting with 0 corresponds to the formula in (3) with the golden mean $\omega = (\sqrt{5}+1)/2$. The parameter J in (2) is fixed with $J = r^{-\rho}$, where

$$\rho = \lim_{L\to\infty} \frac{\sum_{i=1}^{L} f_i}{L} = 1 - \frac{1}{\omega} \tag{4}$$

is the fraction of units 1 in the infinite sequence. Note that $r = 1$ represents the homogeneous lattice.

The essential technique in the solution of $\mathcal{H}$ is the mapping to spinless free fermions [75, 76]. First, we express the spin operators $\sigma_i^{x,y,z}$ in terms of fermion creation (annihilation) operators $c_i^\dagger$ (c_i) by using the Jordan–Wigner transformation [74]: $c_i^\dagger = a_i^+ \exp[\pi\imath \sum_j^{i-1} a_j^+ a_j^-]$ and $c_i = \exp[\pi\imath \sum_j^{i-1} a_j^+ a_j^-] a_i^-$, where $a_j^\pm = (\sigma_j^x \pm \imath\sigma_j^y)/2$. Here and throughout the paper, we denote the imaginary unit $\sqrt{-1}$ by $\imath$ to avoid confusion with the integer index i. The Ising Hamiltonian in (1) can then be written in a quadratic form in fermion operators:

$$\mathcal{H} = -\sum_{i=1}^{L} h\left(c_i^\dagger c_i - \frac{1}{2}\right) - \frac{1}{2}\sum_{i=1}^{L-1} J_i (c_i^\dagger - c_i)(c_{i+1}^\dagger + c_{i+1}) + \frac{1}{2} J_L (c_L^\dagger - c_L)(c_1^\dagger + c_1) \exp(\imath\pi\mathcal{N}), \tag{5}$$

where $\mathcal{N} = \sum_{i=1}^{L} c_i^\dagger c_i$ is the number of fermions. The Hamiltonian (5) can be diagonalized through a canonical transformation [75], in which a new set of fermion operator η_k is introduced by

$$\eta_k = \sum_{i=1}^{L} \left[\frac{1}{2}\left(\Phi_k(i) + \Psi_k(i)\right) c_i + \frac{1}{2}\left(\Phi_k(i) - \Psi_k(i)\right) c_i^\dagger\right], \tag{6}$$

where the $\Phi_k(i)$ and $\Psi_k(i)$ are real, and normalized by

$$\sum_{k=1}^{L} \Phi_k(i)\Phi_k(j) = \sum_{k=1}^{L} \Psi_k(i)\Psi_k(j) = \delta_{ij}. \tag{7}$$

We then obtain the diagonal form of $\mathcal{H}$:

$$\mathcal{H} = \sum_{k=1}^{L} \epsilon_k \left(\eta_k^\dagger \eta_k - \frac{1}{2}\right) \tag{8}$$

in terms of the new fermion creation (annihilation) operators $\eta_k^\dagger$ (η_k). The energies of free fermionic modes, ϵ_k, and the components, $\Phi_k(i)$ and $\Psi_k(i)$, can be obtained from the solutions of the eigenvalue problem:

$$\begin{aligned} \epsilon_k \Psi_k(i) &= -h\Phi_k(i) - J_k \Phi_k(i+1), \\ \epsilon_k \Phi_k(i) &= -J_{k-1}\Psi_k(i-1) - h\Psi_k(i). \end{aligned} \tag{9}$$

The spectrum of free-fermionic excitations, ϵ_k in (8), plays a key role in equilibrium and non-equilibrium properties of the system. In equilibrium and in the thermodynamic limit the model has a quantum critical point at $h = h_c$, the properties of which are controlled by the low-energy excitations. The value of h_c is determined by the equation [76] $\ln h_c = \overline{\ln J}$, where the overbar denotes an average over all sites. With the parameterization given above, the critical point is given by $h_c = 1$, independently of r. The lowest gap, $\Delta E = \epsilon_1$, is zero for $h < h_c$, and vanishes as $\Delta E \sim (h_c - h)^{\nu}$, as h approaches h_c. The singularity of the gap, measured by the gap-exponent $\nu = 1$, does not depend on r; the same is true for the singularity of the specific heat: $C_v \sim \ln|h - h_c|$. Thus the transition belongs to the Onsager [77] universality class, irrespectively of r. This means that the quasiperiodic modulation of the couplings represents an irrelevant perturbation at the critical point of the homogeneous model [78]. For $h < h_c$ the system is in the ordered phase, so that the local magnetization at site l is $m_l > 0$. Upon approaching the critical point, the local magnetization goes to zero following a power law: the bulk magnetization m_b decays as $m_b(h) \sim (h_c - h)^{1/8}$, which defines the critical exponent $\beta_b = 1/8$, while the surface magnetization m_1 vanishes as $m_1(h) \sim (h_c - h)^{\beta_s}$ with $\beta_s = 1/2$. For $h > h_c$ the system is in the disordered phase and the local magnetization vanishes in the thermodynamic limit.

While in equilibrium only the low-energy excitations are of importance, the complete energy spectrum contributes to non-equilibrium properties, which are investigated in this paper.

3. Non-equilibrium properties of homogeneous and random chains

We consider a quench process in which at time $t = 0$ the strength of the transverse field is changed suddenly from h_0 to another value, say h. The initial Hamiltonian with h_0 for $t < 0$ is denoted by $\mathcal{H}_0$, and its ground state is $|\Psi_0^{(0)}\rangle$. For $t > 0$ the new Hamiltonian $\mathcal{H}$ with h governs the coherent time evolution of the system; for example, an observable, represented by the operator $\hat{A}$, has the time evolution in the Heisenberg picture as: $\hat{A}(t) = \exp(\imath t\mathcal{H})\hat{A}\exp(-\imath t\mathcal{H})$, and its expectation value for $t > 0$ is given by $A(t) = \langle\Psi_0^{(0)}|\hat{A}(t)|\Psi_0^{(0)}\rangle$. Dynamics of the system out of equilibrium is governed by the complete spectrum of $\mathcal{H}$ and not only by the lowest excitations. Therefore, Hamiltonians with different spectral properties will have completely different non-equilibrium properties.

The form of the inhomogeneity in the couplings is generally crucial to the spectrum of a Hamiltonian. For example, the spectrum of the homogeneous quantum Ising chain is absolutely continuous; thus all the eigenstates are extended. In contrast, the random chain has a singular point spectrum and the eigenstates are localized. The spectrum of quasiperiodic chains lies between the above-mentioned two limiting cases [79, 80]; for example, the spectrum of the Fibonacci chain defined in (1) is given by a Cantor set of zero Lebesgue measure, signaling that the spectrum is of a multifractal type, and it is called purely singular continuous [81] in the mathematical denotation. See [79] for precise mathematical definitions of different spectra.

Below we first briefly review non-equilibrium properties of the entanglement entropy and local magnetization after a quench in the homogeneous chain and in random chains.

3.1. Entanglement entropy

The *entanglement entropy*, $\mathcal{S}_\ell(t)$, of a block of the first ℓ sites in the chain is defined as $\mathcal{S}_\ell(t) = \mathrm{Tr}_\ell[\rho_\ell(t)\ln\rho_\ell(t)]$ in terms of the reduced density matrix: $\rho_\ell(t) = \mathrm{Tr}_{i>\ell}|\Psi_0(t)\rangle\langle\Psi_0(t)|$.

Here $|\Psi_0(t)\rangle$ denotes the ground state of the complete system at time $t > 0$. The details of the calculation of $S_\ell(t)$ in the free-fermion representation can be found in the appendix of [82].

For the *homogeneous chain* (corresponding to the case with $r = 1$ in (2)) in the limit $L \to \infty$ and for $\ell \gg 1$, the results can be summarized as follows [33, 36]:

$$S_\ell(t) = \begin{cases} \alpha t & t < \ell/v_{\max}, \\ \beta \ell & t \gg \ell/v_{\max}, \end{cases} \tag{10}$$

where $v_{\max}$ is a maximum velocity. For a quench to a quantum critical point, the result in (10) is the consequence of conformal invariance [33]; for the other cases, this behavior can be explained in the framework of a semiclassical (SC) theory [33, 34]: entanglement between the subsystem and its environment arises when two quantum entangled quasiparticles, which are emitted at $t = 0$ and move ballistically with opposite velocities, arrive in both the subsystem and the environment simultaneously. The prefactors $\alpha = \alpha(h_0, h)$ and $\beta = \beta(h_0, h)$ have been exactly calculated [54] and these agree with the results obtained from the SC theory [34]. In [83], $\alpha(h_0 = 0, h)$ has been evaluated in a closed formula, which is a continuous function of h, but at the critical point $h = 1$, its second derivative is logarithmically divergent.

In the *random chain* the excitations are localized and therefore the dynamical entanglement entropy approaches a finite limiting value. When the quench is performed to the random quantum critical point, the average entropy increases ultra-slowly as $\log[\log(t)]$ [36]. This behavior can be explained in terms of the strong disorder renormalization group [36, 39, 84, 85].

3.2. Local magnetization

Another quantity we consider is the *local magnetization*, $m_l(t)$, at a position, l, of an open chain. Following Yang [86], this is defined for large L as the off-diagonal matrix element:

$$m_l(t) = \langle \Psi_0^{(0)} | \sigma_l^x(t) | \Psi_1^{(0)} \rangle, \tag{11}$$

where $|\Psi_1^{(0)}\rangle$ is the first excited state of the initial Hamiltonian. The calculation of the magnetization in terms of free fermions is outlined in the appendix.

For the *homogeneous chain* the time dependence of the local magnetization has been numerically calculated in [34, 58]. For the quench performed within the ordered phases, $h_0 < 1$ and $h < 1$, the results in the limit $L \to \infty$ and $l \gg 1$ are given by

$$m_l(t) \sim \begin{cases} \exp(-t/\tau) & t < l/v_{\max}, \\ \exp(-l/\xi) & t \gg l/v_{\max}, \end{cases} \tag{12}$$

where the relaxation (decoherence) time τ and the correlation length ξ depend on the quench parameters h_0 and h. Exact expressions for these quantities were derived recently [61, 63, 64]. In the small h_0 and h limit, accurate results can also been obtained from the SC theory [34, 87]. In this framework, the quasiparticles in terms of the σ operators are represented by ballistically moving kinks. Each time a kink passes a site l, the σ_l^z operator changes sign; thus kinks that pass a site an even number of times have no effect on the local magnetization. Summing up the contributions of all kinks, we obtain the functional form in (12). If the quench is performed close to the critical point, the kinks have a finite width; this effect can be taken into account in a modified SC theory [34, 65], which provides exact results.

For quenches involving the disordered phase with $h_0 > 1$ and/or $h > 1$, the results obtained numerically [34, 58] or analytically by the form-factor approach [61, 63, 64] indicate that for bulk spins in large systems the first equation of (12) is modified as

$$m_l(t) \simeq A(t) \exp(-t/\tau), \tag{13}$$

where the prefactor $A(t)$ changes sign during the relaxation process, say $A(t) > 0$ for $t_i < t < t_{i+1}$, $A(t) < 0$ for $t_{i+1} < t < t_{i+2}$, etc. The period of these oscillations: $t_{\rm per}(h) \simeq (t_{i+1} - t_i)$ defines a characteristic time scale, which increases and becomes divergent as $h \to 1^+$. This is a signal of a *dynamical phase transition* in the system. The order parameter can be defined as

$$\mathcal{O} = \lim_{t\to\infty} \frac{1}{t} \int_0^t [|A(t')| - A(t')] \mathrm{d}t', \tag{14}$$

which is positive ($\mathcal{O} > 0$) in the oscillatory phase and $\mathcal{O} = 0$ in the non-oscillatory phase.

In a *disordered chain* away from the random quantum critical point the bulk magnetization approaches a finite limiting value, which reflects the localized nature of the excitations. After a quench performed to the critical point, the average bulk magnetization has been found to vanish asymptotically in a very slow way [88], $m_{\rm b}(t) \sim [\ln(t)]^{-A}$, where $A > 0$ is a disorder-dependent constant.

4. The results for quasiperiodic chains

In this section, we present our results for the quasiperiodic quantum Ising chain after a global quench, obtained by numerical calculations based on the free-fermion representation of the model. We concentrate on the Fibonacci chain with the parameter ω defined in (3) being the golden mean. We consider finite chains with a length fixed at a Fibonacci number F_n. We have calculated the entanglement entropy and the local magnetization for system sizes up to $L = F_{17} = 1597$. For the numerical calculation, we solved Hermitian and anti-Hermitian eigenvalue problems, and calculated the complex determinants using the LAPACK routine. For a given set of parameters (h_0, h and r) the time dependence of the entropy or the magnetization of a chain with $L = 1597$ was obtained in about 1 day of CPU time on a 2.5 GHz processor.

Below we present the results for these two quantities separately.

4.1. Entanglement entropy

For a chain of total length F_n with periodic boundary conditions, we have calculated the entanglement entropy S_ℓ between a block of length $\ell = F_{n-2}$ and its environment that has a length of F_{n-1}. Various values of $0 < r < 1$ for the inhomogeneity amplitude were considered. We start our numerical calculations from the fully ordered state with $h_0 = 0$ to a state with $h > 0$ in both the ordered and the disordered phases, as well as at the critical point. The numerical results for $\mathcal{S}_\ell(t) - \mathcal{S}_\ell(0)$ are shown in figure 1. For all the cases considered, $S_\ell(t)$ exhibits two time regimes: in the late-time regime, the entropy is saturated to an L-dependent value, similar to the behavior for the homogeneous chain; in the early-time regime, it increases with time as a power-law form:

$$\mathcal{S}(t) \sim t^\sigma \tag{15}$$

with some exponent $\sigma < 1$. Our numerical results show that the exponent σ depends on the value of the transverse field in the final state, while it does not vary (significantly) with the initial h_0.

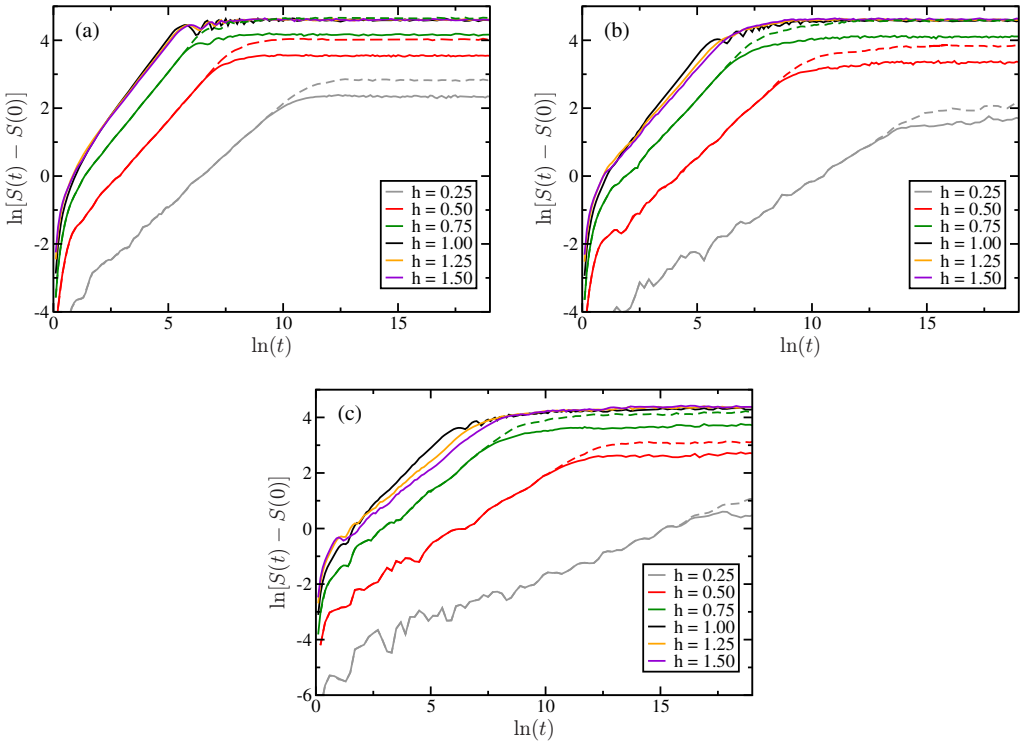

Figure 1. Dynamical entropy after a quench from $h_0 = 0$ to various values of h at the aperiodicity parameters (a) $r = 0.75$, (b) $r = 0.5$ and (c) $r = 0.25$. The solid lines are the results for $L = F_{16} = 987$, and the dashed lines (only at $h = 0.25$, $h = 0.5$ and $h = 0.75$) correspond to the data for $L = F_{17} = 1597$. The 'noise' (irregular variation) present on the curves in the small t regime is due to such low-energy excitations, which are related to the local properties of the quasiperiodic chain and are independent of the chain lengths.

The values of σ for $r = 0.25$, 0.5 and 0.75 are plotted in figure 6; for all the cases considered, σ reaches its maximum at the critical point $h = 1$, and the increase with h in the ordered phase ($h < 1$) is much faster than the decrease in the disordered phase ($h > 1$). Furthermore, we found that the exponent σ decreases with stronger inhomogeneity, that is, with smaller value of r.

The power-law time dependence of the entanglement entropy in (15) is a new feature of the quasiperiodic system: the increase in entropy is slower than in the homogeneous chain, but faster than in a random chain. This behavior can be explained in terms of quasiparticles that are emitted at time $t = 0$, and subsequently move classically by anomalous diffusion, which has a power-law relationship between displacement and time, $x \sim t^D$, with a diffusion exponent $0 < D < 1$. We note that in a homogeneous chain, pairs of quasiparticles that contribute to the entanglement entropy move ballistically (i.e. $x \sim t$) rather than moving by diffusion, which results in the linear growth of the entanglement entropy with time [33] (figure 2). The dynamics of the quasiparticles in our quasiperiodic lattice will be studied in more detail in section 4.3.

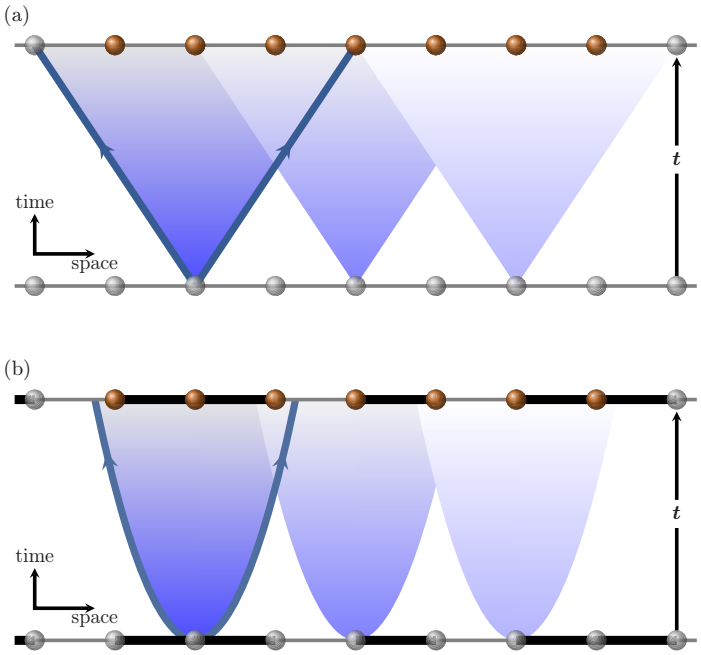

Figure 2. Schematic illustration of the light cones of quasiparticles for a homogeneous quantum Ising chain (a) and for a chain with an aperiodic modulation of the couplings (the thin/thick lines between sites represent weak/strong couplings according to a Fibonacci sequence) (b). The quasiparticle excitations emitted at time $t = 0$ move ballistically in the homogeneous lattice, while their motion is anomalous diffusive with $x \sim t^D$ $(D < 1)$ in the quasiperiodic lattice. Pairs of quasiparticles moving to the left or right from a given point are entangled; they will contribute to the entanglement entropy between a region A (the region with orange sites) and the rest of the chain, region B, if they arrive simultaneously in A and B.

4.2. Local magnetization

The local magnetization, $m_l(t)$, is calculated for open chains of length $L = F_n$. Generally, $m_l(t)$ has a monotonic position dependence: $m_{l_1}(t) > m_{l_2}(t)$ for $l_1 < l_2 < L/2$. We measured the magnetization at site $l = F_{n-1}$, which is considered as the bulk magnetization and denoted by $m_b(t)$. We have also studied the behavior of the surface magnetization, $m_1(t)$, for which some exact results are obtained.

We study the asymptotic behavior of the surface magnetization (given in (A.16)) for large t after a quench. If the quench is performed to the ordered phase, $h < 1$, the lowest excitation energy is $\epsilon_1 = 0$ (i.e. $\cos(\epsilon_1 t) = 1$); consequently, $P_{1,2k-1}(t)$ in (A.7) has a time-independent part. This results in a non-oscillating contribution to the surface magnetization: $\overline{m_1} = \lim_{t\to\infty} \int_0^t m_1(t')\,\mathrm{d}t'$, which is given by

$$\overline{m_1} = \Phi_1(1) \sum_{j=1}^{L} \Phi_1(j)\Phi_1^{(0)}(j) \tag{16}$$

and defines its stationary value. Recall that $\Phi_1(1) = m_1(h, t = 0)$, i.e. it is equal to the equilibrium surface magnetization [89, 90], which is finite for $h < 1$, and zero in the disordered

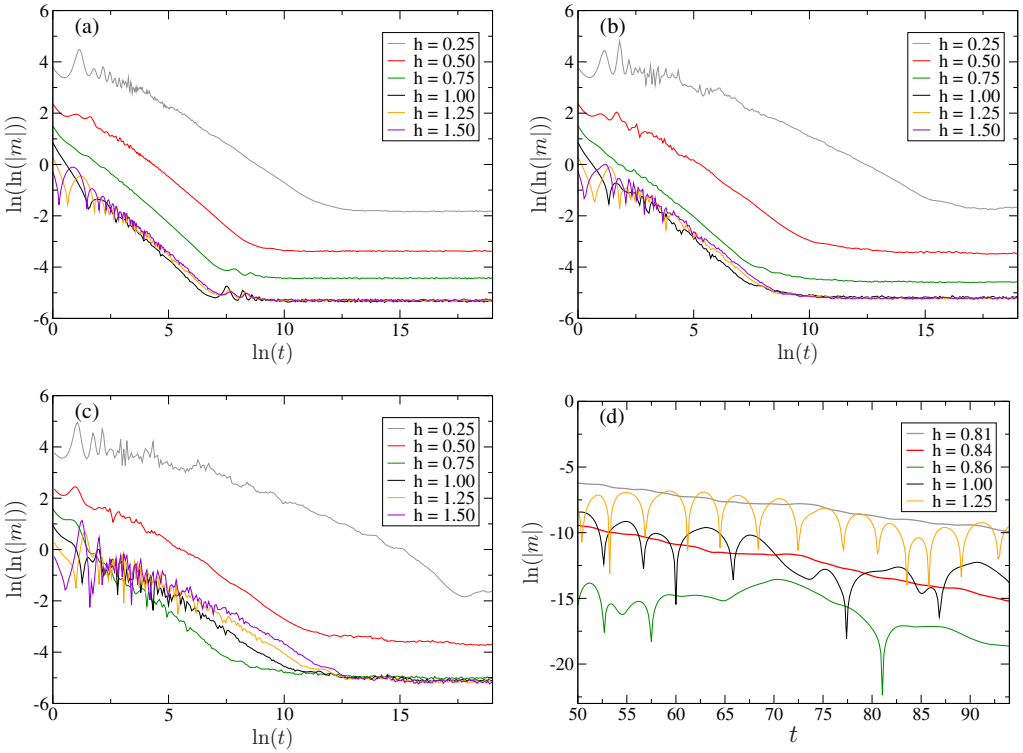

Figure 3. Double logarithm of the bulk magnetization as a function of the logarithm of the time. During the quench the transverse field is changed from $h_0 = 0$ to different values of h at the aperiodicity parameter $r = 0.75$ (a), $r = 0.5$ (b) and $r = 0.25$ (c). The length of the chain is $L = F_{17} = 1597$ and the magnetization is considered at site $l = F_{16} = 987$. In panel (d), $\ln|m_b(t)|$ is shown as a function of t in the window $50 < t < 100$ for different values of h at $r = 0.5$. The oscillations in $\ln|m_b(t)|$ (i.e. in the prefactor $A(t)$) occur when h is larger than a certain value h^* (here $h^* \approx 0.85$), and the oscillations disappear for $h < h^*$; the dynamical phase transition described in the main text occurs at h^*.

phase. Similarly, $\Phi_1^{(0)}(1) > 0$ for $h_0 < 1$ and zero otherwise. From this it follows that the stationary non-equilibrium surface magnetization is $\overline{m_1} > 0$, if both $h < 1$ and $h_0 < 1$. Otherwise the stationary surface magnetization vanishes. If the quench starts from the fully ordered initial state $h_0 = 0$, then $\Phi_1^{(0)}(j) = \delta_{1,j}$ and $\overline{m_1} = \Phi_1^2(1)$; thus we obtain the simple relation

$$\overline{m_1}(h) = [m_1(h, t = 0)]^2, \tag{17}$$

which is generally valid between the stationary value of the non-equilibrium surface magnetization and its equilibrium value. From (17) it follows that the critical exponent β_s^{ne} for the non-equilibrium surface magnetization and the critical exponent β_s for the equilibrium surface magnetization are related as $\beta_s^{ne} = 2\beta_s$. According to (17) and [91], for the Fibonacci chain close to the critical point $h \to h_c = 1$, we have $\overline{m_1}(h) \sim 1 - h^2 = (h_c - h)(h_c + h) \sim h_c - h$; thus $\beta_s^{ne} = 1$.

We numerically calculated the time dependence of the bulk magnetization after a quench from the fully ordered initial state, $h_0 = 0$, to different values of h. For fixed values of the

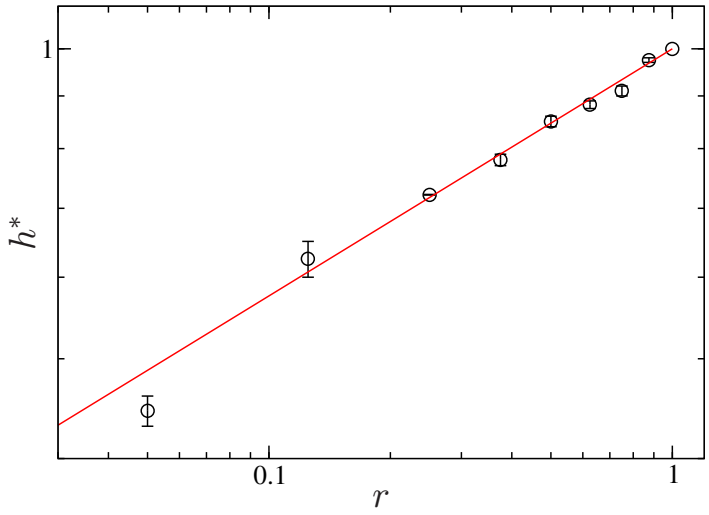

Figure 4. Position of the dynamical critical point for different values of the aperiodicity parameter in a double-logarithmic plot. The straight line has a slope $\alpha = 0.24$.

inhomogeneity $r = 0.25,\ 0.5$ and 0.75, the results for the double logarithm of $|m_b(t)|$ are shown in figures 3(a)–(c) as functions of $\ln t$. In each case one can observe a linear dependence, which implies that the magnetization has asymptotically a stretched exponential time dependence

$$m_b(t) \sim A(t) \exp\left(-Ct^{\mu}\right), \tag{18}$$

which corresponds to equation (13) for a homogeneous system, with $\mu = 1$. Before analyzing the decay exponent μ, we first study the behavior of the prefactor $A(t)$. Like in a homogeneous chain as discussed in section 3.2, there is a dynamical phase transition between a non-oscillating phase for $h < h^*(r)$, where the order-parameter $\mathcal{O}$ defined in (14) is zero, and an oscillating phase for $h > h^*(r)$, where $\mathcal{O} > 0$. In the oscillating phase, the characteristic time scale defined as the period time, $t_{\rm per}(h, r)$, becomes divergent as $h \to h^*(r)^+$. An example of this behavior is illustrated in figure 3, panel (d), in which $\ln|m_b(t)|$ as a function of t is shown in the window $50 < t < 100$ for different values of h at $r = 0.5$; as seen in this figure, the curves for $h = 0.86$, 1.0 and 1.25 oscillate, whereas the oscillations vanish for $h = 0.81$ and 0.84. We identify the dynamical phase transition point as $h^* = 0.850(5)$. In this quasiperiodic model the dynamical phase transition does not coincide with the equilibrium phase transition, since $h^*(r) < 1$ for $r < 1$. Estimates of $h^*(r)$ versus r are shown in figure 4; the data are well approximated by a power law $h^*(r) \sim r^{\alpha}$ with $\alpha = 0.24(3)$.[4]

The exponent μ describing the decay of the local magnetization depends on both h and r; by contrast, it does not vary significantly with h_0, at least for $h_0 < h$. Our results for the critical exponents $\mu = \mu(h, r)$ are plotted in figure 6 for $r = 0.75,\ 0.5$ and 0.25 as functions of h. The exponent μ reaches its maximum at the dynamical phase transition point $h^*(r)$.

[4] No oscillation of the magnetization is expected if all sites are 'locally' in the ferromagnetic phase. This condition is satisfied for a weakly coupled site having one strong (J_s) and one weak (J_w) bond and if $\ln h < \ln J_s + \ln J_w$, which means that $h < r^{2/\omega-1}$. The numerical results in figure 4 indicate that the critical value $h^*(r)$ coincides with $r^{2/\omega-1}$.

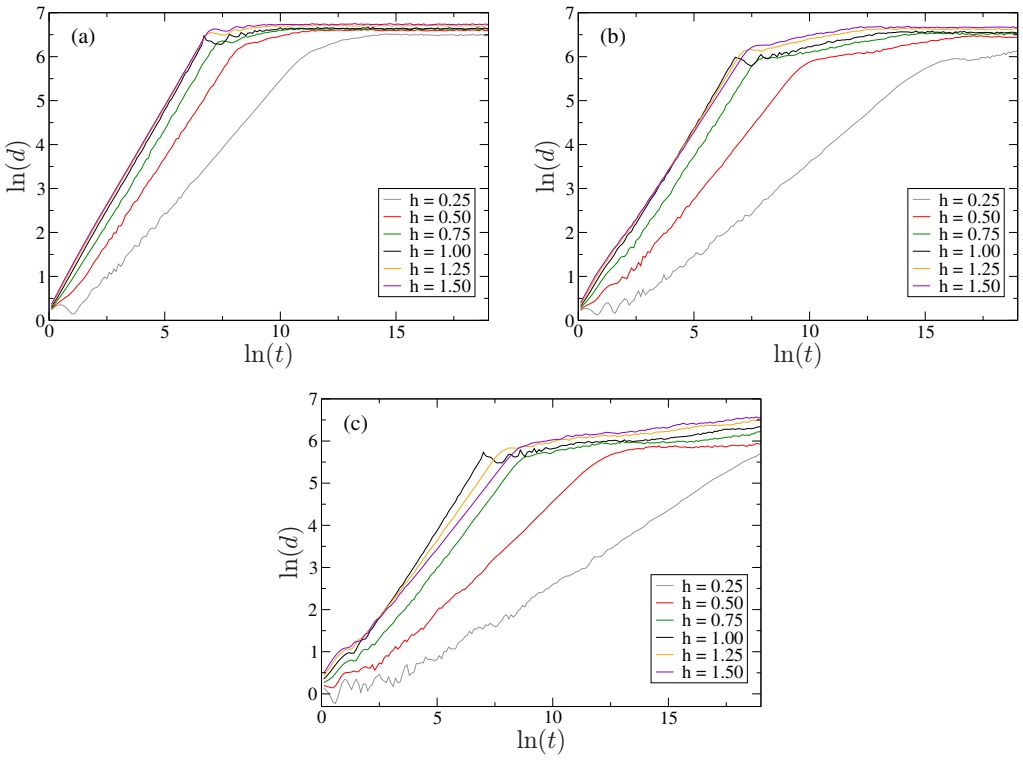

Figure 5. Time-dependent width of the wave packet at different values of h for $r = 0.75$ (a), $r = 0.5$ (b) and $r = 0.25$ (c).

4.3. Interpretation by wave packet dynamics

As is known from previous studies on the homogeneous chain, dynamical features of the entanglement entropy and the local magnetization can be well described by the dynamics of quasiparticles. To understand the dynamical properties of the quasiparticles emitted after a quantum quench in the quasiperiodic lattice, we regard the quasiparticles as wave packets and study their dynamics using a method that has been applied to studies of transport properties of quasicrystals [44, 92].

We construct a wave packet connecting sites k and l at time t in the form

$$W_{l,k}(t) = \frac{1}{2}\sum_q \{\cos(\epsilon_q t)[\Phi_q(l)\Phi_q(k) + \Psi_q(l)\Psi_q(k)] - \imath\,\sin(\epsilon_q t)[\Phi_q(l)\Psi_q(k) + \Phi_q(k)\Psi_q(l)]\}, \tag{19}$$

which is localized at $t = 0$ since $W_{l,k}(0) = \delta_{l,k}$ (cf equation (7)). For a Hamiltonian with eigenfunctions $\phi_q(l)$ and eigenvalues ϵ_q, a wave packet can be obtained by $W_{l,k}(t) = \sum_q \cos(\epsilon_q t)\phi_q(l)\phi_q(k)$, which corresponds to the first term in (19). We note that (19) is just a linear combination of the four time-dependent factors in (A.7), which describe the time dependence of the fermion operators. The width of the wave packet starting from site k after time t is given by

$$d(k,t) = \left[\sum_l (k-l)^2 |W_{l,k}(t)|^2\right]^{\frac{1}{2}}. \tag{20}$$

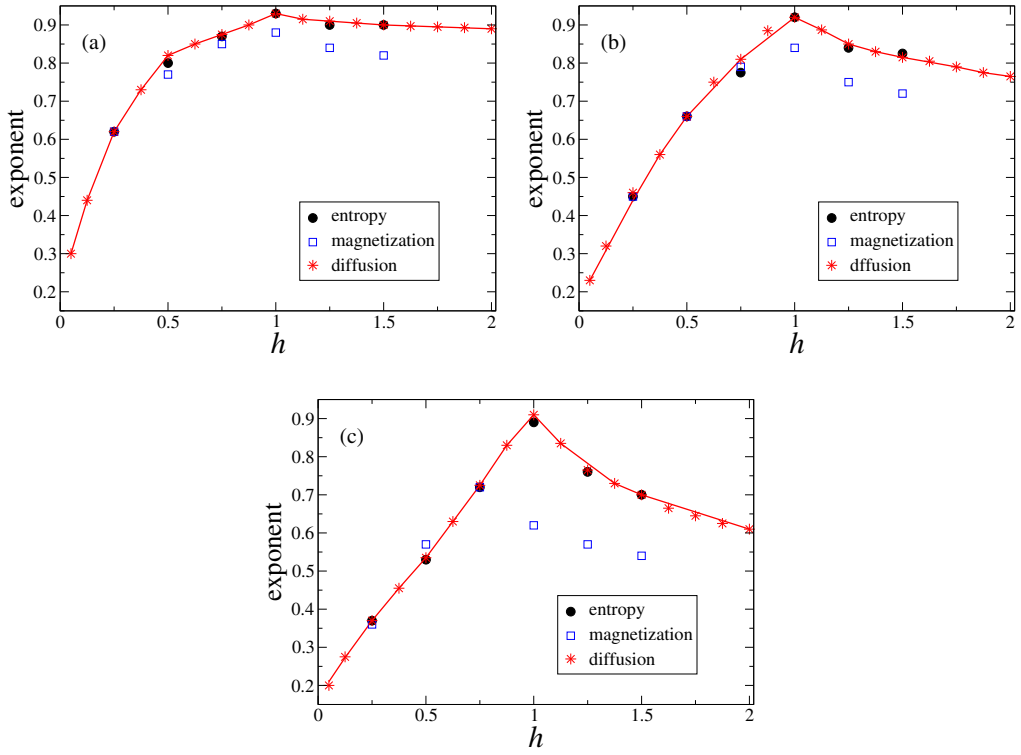

Figure 6. Scaling exponents calculated from the time dependence of the width of the wave packet, from the entanglement entropy and from the magnetization at different values of h for $r = 0.75$ (a), $r = 0.5$ (b) and $r = 0.25$ (c). The full lines connecting the diffusion exponents are a guide to the eye.

The spreading of a wave packet in a perfect crystal with an absolutely continuous energy spectrum is known to be ballistic, i.e. the width increases linearly in time. A heuristic argument is the following [93]: the energy scale $\Delta\epsilon$ defined by the typical variation of the energy levels is proportional to the inverse of the time that a wave packet needs to spread over the chain. In the case of the absolutely continuous spectrum, we have $\Delta\epsilon \sim L^{-1}$, which gives $d \sim L \sim t$. In the case of a singular continuous spectrum as for our quasiperiodic lattice, there are many energy scales $\Delta\epsilon \sim L^{-1/\alpha}$ with a number of exponents α. One then expects that for large t the wave packet in the infinite quasiperiodic lattice shows anomalous diffusion in the form $d(k, t) \sim t^{D(k)}$ with a diffusion exponent $D(k)$, which may depend on the starting position. Here we determine the value of $D(k)$ numerically.

After a global quench, quasiparticles are emitted everywhere in lattices; therefore $d(k, t)$ should be averaged over different initial positions

$$d(t) = \overline{d(k, t)} \sim t^{D}. \tag{21}$$

In our numerical calculations chains of length $L = F_{17} = 1597$ with periodic boundary conditions were considered. First we have confirmed that the wave packet constructed in our method moves ballistically in the homogeneous chain (with $r = 1$), corresponding to $D = 1$. In the quasiperiodic chains the motion is indeed anomalous diffusive with $D < 1$, which is seen in figure 5 where the average widths of the wave packet are presented as functions of time in a

log–log plot for various values of h and $r = 0.75,\ 0.5$ and 0.25. The diffusion exponent D for given h and r corresponds to the slope of the linear part of the function.

The variation of D with h at a fixed r is shown in figure 6, compared with the exponent σ for the entanglement entropy and the exponent μ for the local magnetization. Here one can observe that the agreement between these three exponents is very good for $h < h^*(r)$, i.e. in the non-oscillating phase, but the exponent for the magnetization deviates in the oscillating phase ($h > h^*(r)$). The discrepancy in the oscillating phase implies that the SC picture breaks down in the oscillating phase, where the quasiparticles cannot be well described by the moving kinks in the magnetization.

5. Discussion

In this paper, we have studied the non-equilibrium dynamics of quasiperiodic quantum Ising chains after a global quench. In a quench process, the complete spectrum of the Hamiltonian is relevant for the time evolution of various observables. For the quasiperiodic quantum Ising chain the spectrum is in a very special form, which is given by a Cantor set of zero Lebesgue measure, i.e. purely singular continuous. We have calculated numerically two quantities: the dynamical entanglement entropy and the relaxation of the local magnetization. The entanglement entropy is found to increase in time as a power law (see (15)), whereas the bulk magnetization decays in a stretched exponential way (see (18)). Both behaviors can be explained in a quasiparticle picture, in which the quasiparticles move by anomalous diffusion in the quasiperiodic lattice. The diffusion exponent has been calculated by a wave packet approach, and good agreement with the exponents we obtained for the entropy and for the magnetization has been found. We note that the anomalous dynamics found in the global quench process is similar to the transport properties of quasicrystals.

Relaxation of the bulk magnetization is found to present a non-equilibrium dynamical phase transition. The non-oscillating phase, in which the magnetization is always positive, and the oscillating phase, in which the sign of the magnetization varies periodically in time, are separated by a dynamical phase transition point, at which the time scale of oscillations diverges. This singularity point, due to collective dynamical effects, is different from the equilibrium critical point.

A similar non-equilibrium dynamical behavior is expected to hold for other quasiperiodic or aperiodic quantum models as long as the spectrum of the Hamiltonian is also purely singular continuous; there is a large class of such models, for example the Thue–Morse quantum Ising chain. If, however, the spectrum of the Hamiltonian of the model is in a different type, such as the Harper potential which has extended or localized states, the non-equilibrium dynamics is expected to be different from the case we consider in this paper.

Acknowledgments

FI is grateful to D Karevski, H Rieger and A Sütő for discussions. FI acknowledges support from the Hungarian National Research Fund under grant numbers OTKA K75324 and K77629; he also acknowledges travel support from the National Science Council (NSC), Taiwan, under grant number 101-2912-I-004-518. YCL is supported by the NSC under grants numbers

NSC 98-2112-M-004-002-MY3, NSC 101-2112-M-004-005-MY3 and NSC 100-2923-M-004-002-MY3; she also gratefully acknowledges support from the National Center for Theoretical Sciences of Taiwan.

Appendix. Free-fermionic calculation of the time-dependent local magnetization

To calculate the local magnetization in (11), we need to first calculate the time dependence of the spin operator $\sigma_l^x(t)$ at site l in the Heisenberg picture. We introduce at each site two Majorana fermion operators, $\check{a}_{2l-1}$ and $\check{a}_{2l}$, defined in terms of the free fermion operators $\eta_k^\dagger$ and η_k (given in (6)) as

$$\begin{aligned}\check{a}_{2l-1} &= \sum_{k=1}^{L} \Phi_k(l)(\eta_k^\dagger + \eta_k),\\ \check{a}_{2l} &= -\imath \sum_{k=1}^{L} \Psi_k(l)(\eta_k^\dagger - \eta_k).\end{aligned} \tag{A.1}$$

These satisfy the commutation relations

$$\check{a}_l^\dagger = \check{a}_l, \quad \{\check{a}_l, \check{a}_k\} = 2\delta_{l,k}. \tag{A.2}$$

The spin operators are then expressed in terms of the Majorana operators as

$$\sigma_l^x = \imath^{l-1} \prod_{j=1}^{2l-1} \check{a}_j \tag{A.3}$$

and the local magnetization in (11) is then given as the expectation value of the product of fermion operators with respect to the ground state

$$m_l(t) = (\imath)^{l-1} \left\langle \Psi_0^{(0)} | \prod_{j=1}^{2l-1} \check{a}_j(t)\eta_1 | \Psi_0^{(0)} \right\rangle, \tag{A.4}$$

where we have used $|\Psi_1^{(0)}\rangle = \eta_1|\Psi_0^{(0)}\rangle$. The expression in (A.4)—according to Wick's theorem—can be expressed as a sum of products of two-operator expectation values. This can be written in the compact form of a Pfaffian, which in turn can be evaluated as the square root of the determinant of an antisymmetric matrix:

$$\begin{aligned} m_l(t) &= (-\imath)^{l-1} \begin{vmatrix} \langle \check{a}_1(t)\check{a}_2(t)\rangle & \langle \check{a}_1(t)\check{a}_3(t)\rangle & \cdots & \langle \check{a}_1(t)\check{a}_{2l-1}(t_1)\rangle & \langle \check{a}_1(t)\eta_1\rangle \\ & \langle \check{a}_2(t)\check{a}_3(t)\rangle & \cdots & \langle \check{a}_2(t)\check{a}_{2l-1}(t)\rangle & \langle \check{a}_2(t)\eta_1\rangle \\ & \ddots & & & \vdots \\ & & & \langle \check{a}_{2l-2}(t)\check{a}_{2l-1}(t)\rangle & \langle \check{a}_{2l-2}(t)\eta_1\rangle \\ & & & & \langle \check{a}_{2l-1}(t)\eta_1\rangle \end{vmatrix} \\ &= \pm \left[\det C_{ij}\right]^{1/2}, \end{aligned} \tag{A.5}$$

where C_{ij} is the antisymmetric matrix $C_{ij} = -C_{ji}$, with the elements of the Pfaffian (A.5) above the diagonal. (Here and in the following, we use the shorthand notation: $\langle \cdots \rangle = \langle \Psi_0^{(0)}| \cdots |\Psi_0^{(0)}\rangle$.)

Below we describe how the time evolution of the spin operator σ_l^x follows from the time dependence of the Majorana fermion operators. Inserting $\eta_k^\dagger(t) = \mathrm{e}^{\imath t\epsilon_k}\eta_k^\dagger$ and $\eta_k(t) = \mathrm{e}^{-\imath t\epsilon_k}\eta_k$ into (A.1), one obtains

$$\check{a}_m(t) = \sum_{n=1}^{2L} P_{m,n}(t)\check{a}_n \tag{A.6}$$

with

$$\begin{aligned} P_{2l-1,2k-1} &= \sum_q \cos(\epsilon_q t)\Phi_q(l)\Phi_q(k), \\ P_{2l-1,2k} &= -\sum_q \sin(\epsilon_q t)\Phi_q(l)\Psi_q(k), \\ P_{2l,2k-1} &= \sum_q \sin(\epsilon_q t)\Phi_q(k)\Psi_q(l), \\ P_{2l,2k} &= \sum_q \cos(\epsilon_q t)\Psi_q(l)\Psi_q(k). \end{aligned} \tag{A.7}$$

The two-operator expectation values are given by

$$\langle \check{a}_m(t)\check{a}_n(t)\rangle = \sum_{k_1,k_2} P_{m,k_1}(t)P_{n,k_2}(t)\langle \check{a}_{k_1}\check{a}_{k_2}\rangle. \tag{A.8}$$

The *equilibrium* correlations in the initial state with a transverse field h_0 are

$$\begin{aligned} \langle \check{a}_{2m-1}\check{a}_{2n-1}\rangle &= \langle \check{a}_{2m}\check{a}_{2n}\rangle \quad = \delta_{m,n}, \\ \langle \check{a}_{2m-1}\check{a}_{2n}\rangle &= -\langle \check{a}_{2m}\check{a}_{2n-1}\rangle = \imath G^{(0)}_{n,m}, \end{aligned} \tag{A.9}$$

where the static correlation matrix $G^{(0)}_{m,n}$ is given by

$$G^{(0)}_{m,n} = -\sum_q \Psi_q^{(0)}(m)\Phi_q^{(0)}(n), \tag{A.10}$$

where $\Psi_q^{(0)}(m)$ and $\Phi_q^{(0)}(n)$ are the components of the eigenvectors in (9), calculated for the initial Hamiltonian. Then (A.8) can be written in the form

$$\langle \check{a}_m(t)\check{a}_n(t)\rangle = \delta_{m,n} + \imath\Gamma_{m,n}(t) \tag{A.11}$$

with

$$\begin{aligned} \Gamma_{2l-1,2m-1} &= \sum_{k_1,k_2}\left[G^{(0)}_{k_2,k_1}P_{2l-1,2k_1-1}P_{2m-1,2k_2} - G^{(0)}_{k_1,k_2}P_{2l-1,2k_1}P_{2m-1,2k_2-1}\right], \\ \Gamma_{2l-1,2m} &= \sum_{k_1,k_2}\left[G^{(0)}_{k_2,k_1}P_{2l-1,2k_1-1}P_{2m,2k_2} - G^{(0)}_{k_1,k_2}P_{2l-1,2k_1}P_{2m,2k_2-1}\right], \\ \Gamma_{2l,2m-1} &= -\sum_{k_1,k_2}\left[G^{(0)}_{k_2,k_1}P_{2l,2k_2}P_{2m-1,2k_1-1} - G^{(0)}_{k_1,k_2}P_{2l,2k_2-1}P_{2m-1,2k_1}\right], \\ \Gamma_{2l,2m} &= \sum_{k_1,k_2}\left[G^{(0)}_{k_2,k_1}P_{2l,2k_1-1}P_{2m,2k_2} - G^{(0)}_{k_1,k_2}P_{2l,2k_1}P_{2m,2k_2-1}\right]. \end{aligned} \tag{A.12}$$

In (A.5) there are also the contractions

$$\begin{aligned}\Pi_m &= \langle\Psi_0^{(0)}|\check{a}_m(t)\eta_1|\Psi_0^{(0)}\rangle \\ &= \sum_n P_{m,n}\langle\Psi_0^{(0)}|\check{a}_n\eta_1|\Psi_0^{(0)}\rangle,\end{aligned} \tag{A.13}$$

where

$$\begin{aligned}\langle\Psi_0^{(0)}|\check{a}_{2l-1}\eta_1|\Psi_0^{(0)}\rangle &= \Phi_1^{(0)}(l), \\ \langle\Psi_0^{(0)}|\check{a}_{2l}\eta_1|\Psi_0^{(0)}\rangle &= \imath\,\Psi_1^{(0)}(l).\end{aligned} \tag{A.14}$$

Thus, finally the square of the local magnetization is given by the determinant

$$m_l^2(t) = \begin{vmatrix} 0 & \Gamma_{1,2} & \Gamma_{1,3} & \cdots & \Gamma_{1,2l-1} & \Pi_1 \\ -\Gamma_{1,2} & 0 & \Gamma_{2,3} & \cdots & \Gamma_{2,2l-1} & \Pi_2 \\ -\Gamma_{1,3} & -\Gamma_{2,3} & 0 & \cdots & \Gamma_{3,2l-1} & \Pi_3 \\ & & & \ddots & \vdots & \\ -\Gamma_{1,2l-1} & \cdots & & 0 & \Pi_{2l-1} & \\ -\Pi_1 & \cdots & & -\Pi_{2l-1} & 0 & \end{vmatrix}. \tag{A.15}$$

As a special case, the surface magnetization is expressed as

$$m_1(t) = \Pi_1 = \sum_{j=1}^{L} P_{1,2j-1}(t)\Phi_1^{(0)}(j) - \imath \sum_{j=1}^{L} P_{1,2j}(t)\Psi_1^{(0)}(j). \tag{A.16}$$

References

[1] Greiner M, Mandel O, Hänsch T W and Bloch I 2002 *Nature* **419** 51
[2] Paredes B *et al* 2004 *Nature* **429** 277
[3] Kinoshita T, Wenger T and Weiss D S 2004 *Science* **305** 1125
[4] Sadler L E, Higbie J M, Leslie S R, Vengalattore M and Stamper-Kurn D M 2006 *Nature* **443** 312
[5] Lamacraf A 2006 *Phys. Rev. Lett.* **98** 160404
[6] Kinoshita T, Wenger T and Weiss D S 2006 *Nature* **440** 900
[7] Hofferberth S, Lesanovsky I, Fischer B, Schumm T and Schmiedmayer J 2007 *Nature* **449** 324
[8] Trotzky S, Chen Y-A, Flesch A, McCulloch I P, Schollwöck U, Eisert J and Bloch I 2012 *Nature Phys.* **8** 325
[9] Cheneau M, Barmettler P, Poletti D, Endres M, Schauss P, Fukuhara T, Gross C, Bloch I, Kollath C and Kuhr S 2012 *Nature* **481** 484
[10] Gring M, Kuhnert M, Langen T, Kitagawa T, Rauer B, Schreitl M, Mazets I, Smith D A, Demler E and Schmiedmayer J 2012 *Science* **337** 1318
[11] Polkovnikov A, Sengupta K, Silva A and Vengalattore M 2011 *Rev. Mod. Phys.* **83** 863
[12] Rigol M, Dunjko V, Yurovsky V and Olshanii M 2007 *Phys. Rev. Lett.* **98** 50405
Rigol M, Dunjko V and Olshanii M 2008 *Nature* **452** 854
[13] Calabrese P and Cardy J 2006 *Phys. Rev. Lett.* **96** 136801
[14] Calabrese P and Cardy J 2007 *J. Stat. Mech.* P06008
[15] Cazalilla M A 2006 *Phys. Rev. Lett.* **97** 156403
Iucci A and Cazalilla M A 2009 *Phys. Rev.* A **80** 063619
Iucci A and Cazalilla M A 2010 *New J. Phys.* **12** 055019
[16] Manmana S R, Wessel S, Noack R M and Muramatsu A 2007 *Phys. Rev. Lett.* **98** 210405

[17] Cramer M, Dawson C M, Eisert J and Osborne T J 2008 *Phys. Rev. Lett.* **100** 030602
Cramer M and Eisert J 2010 *New J. Phys.* **12** 055020
Cramer M, Flesch A, McCulloch I A, Schollwöck U and Eisert J 2008 *Phys. Rev. Lett.* **101** 063001
Flesch A, Cramer M, McCulloch I P, Schollwöck U and Eisert J 2008 *Phys. Rev.* A **78** 033608
[18] Barthel T and Schollwöck U 2008 *Phys. Rev. Lett.* **100** 100601
[19] Kollar M and Eckstein M 2008 *Phys. Rev.* A **78** 013626
[20] Sotiriadis S, Calabrese P and Cardy J 2009 *Europhys. Lett.* **87** 20002
[21] Roux G 2009 *Phys. Rev.* A **79** 021608
Roux G 2010 *Phys. Rev.* A **81** 053604
[22] Sotiriadis S, Fioretto D and Mussardo G 2012 *J. Stat. Mech.* P02017
Fioretto D and Mussardo G 2010 *New J. Phys.* **12** 055015
Brandino G P, De Luca A, Konik R M and Mussardo G 2012 *Phys. Rev.* B **85** 214435
[23] Kollath C, Läuchli A and Altman E 2007 *Phys. Rev. Lett.* **98** 180601
Biroli G, Kollath C and Läuchli A 2010 *Phys. Rev. Lett.* **105** 250401
[24] Banuls M C, Cirac J I and Hastings M B 2011 *Phys. Rev. Lett.* **106** 050405
[25] Gogolin C, Müller M P and Eisert J 2011 *Phys. Rev. Lett.* **106** 040401
[26] Rigol M and Fitzpatrick M 2011 *Phys. Rev.* A **84** 033640
[27] Caneva T, Canovi E, Rossini D, Santoro G E and Silva A 2011 *J. Stat. Mech.* P07015
[28] Cazalilla M A, Iucci A and Chung M-C 2012 *Phys. Rev.* E **85** 011133
[29] Rigol M and Srednicki M 2012 *Phys. Rev. Lett.* **108** 110601
[30] Santos L F, Polkovnikov A and Rigol M 2011 *Phys. Rev. Lett.* **107** 040601
[31] Grisins P and Mazets I E 2011 *Phys. Rev.* A **84** 053635
[32] Canovi E, Rossini D, Fazio R, Santoro G E and Silva A 2011 *Phys. Rev.* B **83** 094431
[33] Calabrese P and Cardy J 2005 *J. Stat. Mech.* P04010
[34] Rieger H and Iglói F 2011 *Phys. Rev.* B **84** 165117
[35] De Chiara G, Montangero S, Calabrese P and Fazio R 2006 *J. Stat. Mech.* L03001
[36] Iglói F, Szatmári Z and Lin Y-C 2012 *Phys. Rev.* B **85** 094417
[37] Levine G C, Bantegui M J and Burg J A 2012 *Phys. Rev.* B **86** 174202
[38] Bardarson J H, Pollmann F and Moore J E 2012 *Phys. Rev. Lett.* **109** 017202
[39] Vosk R and Altman E 2013 *Phys. Rev. Lett.* **110** 067204
[40] Shechtman D, Blech I, Gratias D and Cahn J W 1984 *Phys. Rev. Lett.* **53** 1951
[41] Dubois J-M 2005 *Useful Quasicrystals* (Singapore: World Scientific)
[42] Penrose R 1974 *Bull. Inst. Math. Appl.* **10** 266
[43] Stadnik Z M 1999 *Physical Properties of Quasicrystals* (Berlin: Springer)
[44] Roche S, Trambly de Laissardiére G and Mayou D 1997 *J. Math. Phys.* **38** 1794
Mayou D, Berger C, Cyrot-Lackmann F, Klein T and Lanco P 1993 *Phys. Rev. Lett.* **70** 3915
[45] Roati G, D'Errico C, Fallani L, Fattori M, Fort C, Zaccanti M, Modugno G, Modugno M and Inguscio M 2008 *Nature* **453** 895
[46] Deissler B, Lucioni E, Modugno M, Roati G, Tanzi L, Zaccanti M, Inguscio M and Modugno G 2011 *New J. Phys.* **13** 023020
[47] Harper P G 1955 *Proc. Phys. Soc.* A **68** 874
[48] Aubry S and André G 1980 *Ann. Isr. Phys. Soc.* **3** 133
[49] Modugno M 2009 *New J. Phys.* **11** 033023
[50] Gramsch C and Rigol M 2012 *Phys. Rev.* A **86** 053615
[51] Barouch E, McCoy B and Dresden M 1970 *Phys. Rev.* A **2** 1075
Barouch E and McCoy B 1971 *Phys. Rev.* A **3** 786
Barouch E and McCoy B 1971 *Phys. Rev.* A **3** 2137
[52] Iglói F and Rieger H 2000 *Phys. Rev. Lett.* **85** 3233
[53] Sengupta K, Powell S and Sachdev S 2004 *Phys. Rev.* A **69** 053616

[54] Fagotti M and Calabrese P 2008 *Phys. Rev.* A **78** 010306
[55] Silva A 2008 *Phys. Rev. Lett.* **101** 120603
Gambassi A and Silva A 2011 arXiv:1106.2671
[56] Rossini D, Silva A, Mussardo G and Santoro G 2009 *Phys. Rev. Lett.* **102** 127204
Rossini D, Suzuki S, Mussardo G, Santoro G E and Silva A 2010 *Phys. Rev.* B **82** 144302
[57] Campos Venuti L and Zanardi P 2010 *Phys. Rev.* A **81** 022113
Campos Venuti L, Jacobson N T, Santra S and Zanardi P 2011 *Phys. Rev. Lett.* **107** 010403
[58] Iglói F and Rieger H 2011 *Phys. Rev. Lett.* **106** 035701
[59] Divakaran U, Iglói F and Rieger H 2011 *J. Stat. Mech.* P10027
[60] Foini L, Cugliandolo L F and Gambassi A 2011 *Phys. Rev.* B **84** 212404
Foini L, Cugliandolo L F and Gambassi A 2012 *J. Stat. Mech.* P09011
[61] Calabrese P, Essler F H L and Fagotti M 2011 *Phys. Rev. Lett.* **106** 227203
[62] Schuricht D and Essler F H L 2012 *J. Stat. Mech.* P04017
[63] Calabrese P, Essler F H L and Fagotti M 2012 *J. Stat. Mech.* P07016
[64] Calabrese P, Essler F H L and Fagotti M 2012 *J. Stat. Mech.* P07022
[65] Blaß B, Rieger H and Iglói F 2012 *Europhys. Lett.* **99** 30004
[66] Essler F H L, Evangelisti S and Fagotti M 2012 *Phys. Rev. Lett.* **109** 247206
[67] Iglói F 1988 *J. Phys. A: Math. Gen.* **21** L911
Doria M M and Satija I I 1988 *Phys. Rev. Lett.* **60** 444
Ceccatto H A 1989 *Phys. Rev. Lett.* **62** 203
Ceccatto H A 1989 *Z. Phys.* B **75** 253
Benza G V 1989 *Europhys. Lett.* **8** 321
Henkel M and Patkós A 1992 *J. Phys. A: Math. Gen.* **25** 5223
[68] Turban L, Iglói F and Berche B 1994 *Phys. Rev.* B **49** 12695
[69] Iglói F and Turban L 1996 *Phys. Rev. Lett.* **77** 1206
[70] Iglói F, Turban L, Karevski D and Szalma F 1997 *Phys. Rev.* B **56** 11031
[71] Hermisson J, Grimm U and Baake M 1997 *J. Phys. A: Math. Gen.* **30** 7315
[72] Hermisson J 2000 *J. Phys. A: Math. Gen.* **33** 57
[73] Iglói F, Juhász R and Zimborás Z 2007 *Europhys. Lett.* **79** 37001
[74] Jordan P and Wigner E 1928 *Z. Phys.* **47** 631
[75] Lieb E, Schultz T and Mattis D 1961 *Ann. Phys., NY* **16** 407
Pfeuty P 1970 *Ann. Phys., Paris* **57** 79
[76] Pfeuty P 1979 *Phys. Lett.* **72A** 245
[77] Onsager L 1944 *Phys. Rev.* **65** 117
[78] Luck J M 1993 *Europhys. Lett.* **24** 359
Iglói F 1993 *J. Phys. A: Math. Gen.* **26** L703
[79] Sütő A 1995 *Beyond Quasicrystals* ed F Axel and D Gratias (Berlin: Springer) p 481
[80] Damanik D 2000 *J. Math. Anal. Appl.* **249** 393
Damanik D and Gorodetski A 2011 *Commun. Math. Phys.* **205** 221
[81] Yessen W N 2012 arXiv:1203.2221
[82] Iglói F, Szatmári Z and Lin Y-C 2009 *Phys. Rev.* B **80** 024405
[83] Eisler V, Iglói F and Peschel I 2009 *J. Stat. Mech.* P02011
[84] Fisher D S 1995 *Phys. Rev.* B **51** 6411
[85] For a review see Iglói F and Monthus C 2005 *Phys. Rep.* **412** 277
[86] Yang C N 1952 *Phys. Rev.* **85** 808
[87] Sachdev A and Young A P 1997 *Phys. Rev. Lett.* **78** 2220
[88] Iglói F 2013 in preparation
[89] Peschel I 1984 *Phys. Rev.* B **30** 6783
[90] Iglói F and Rieger H 1998 *Phys. Rev.* B **57** 4238

[91] Iglói F, Rieger H and Turban L 1999 *Phys. Rev.* E **59** 1465
[92] Poon S J 1992 *Adv. Phys.* **41** 303
Yuan H Q, Grimm U, Repetowicz P and Schreiber M 2000 *Phys. Rev.* B **62** 15569
Schulz-Baldes H and Bellissard J 1998 *Rev. Math. Phys.* **10** 1
Huckestein B and Schweitzer L 1994 *Phys. Rev. Lett.* **72** 713
Thiem S and Schreiber M 2012 *Phys. Rev.* B **85** 224205
[93] Thouless D J 1977 *Phys. Rev. Lett.* **39** 1167
Piéchon F 1996 *Phys. Rev. Lett.* **76** 4372